Supporting Information

Zirconium Fluoride-Supported High-Entropy Fluoride: A Catalyst for Enhanced Oxygen Evolution Reaction

Christian Heinekamp,[a,b] Arkendu Roy,[a,b] Stephanos Karafiludis,[a,b] Sourabh Kumar,[a] Ana Guilherme Buzanich,[a] Tomasz M. Stawski,[a] Aistė Miliūtė,[a,b] Marcus on der Au,[a] Mike Ahrens,[b] Thomas Braun,*[b] and Franziska Emmerling*[a,b]

[a.] Department Materials Chemistry, Federal Institute for Material Research and Testing, Richard-Willstätter-Straße 11, 12489 Berlin
E-mail: *franziska.emmerling@bam.de*
[b.] Department of Chemistry, Humboldt Universität zu Berlin, Brook-Taylor-Straße 2, 12489 Berlin
E-Mail: *thomas.braun@cms.hu-berlin.de*

Table of Contents

Reaction scheme for the synthesis of the catalyst

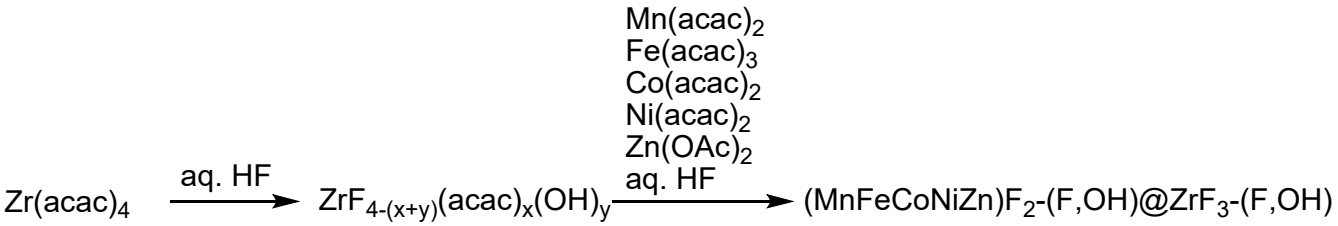

Scheme 1: Reaction scheme for the synthesis of the catalyst.

Elemental analysis using ICP-MS

Table S1: Instrumental settings of the ICP-MS instrument used for quantification.

Parameter	**ICAP-Q (Thermo Scientific)**
Sample introduction	Spray chamber
Nebulizer	PFA – 100 µL (Elemental Scientific)
Interface	Ni skimmer + sampler
RF power (W)	1550
Nebulizer gas (L min^{-1})	1.11
Auxillery gas (L min^{-1})	0.65
Isotopes	^{24}Mg, ^{25}Mg, ^{52}Cr, ^{53}Cr, ^{54}Fe, ^{55}Mn, ^{57}Fe, ^{59}Co, ^{60}Ni, ^{61}Ni, ^{62}Ni ^{63}Cu, ^{65}Cu, ^{66}Zn, ^{67}Zn, ^{68}Zn, ^{89}Y, ^{91}Zr, ^{92}Zr, ^{94}Zr, ^{96}Zr, ^{115}In
Dwell time (s)	0.01
Sweeps	20
Runs	5

Table S2: Elemental composition obtained from ICP-MS. Percentages are normalised to the sum of the six metals. Standard deviation is obtained from six measurements.

Mn	Fe	Co
3%	3%	3%
11.1±0.00mg g^{-1}	11.2±0.5mg g^{-1}	12.5±0.1mg g^{-1}
Ni	Zn	Zr
3%	3%	85%
13.0±0.3mg g^{-1}	14.9±0.1mg g^{-1}	370.4±2.2mg g^{-1}

Table S3: Elemental composition obtained from ICP-MS of the electrolyte after an 1h OER experiment.

Mn	Fe	Co
<6 ng mL^{-1}	<250 ng mL^{-1}	4±1 ng mL^{-1}
Ni	Zn	Zr
<3 ng mL^{-1}	85±17 ng mL^{-1}	89±18 ng mL^{-1}

TEM Images of the HEF

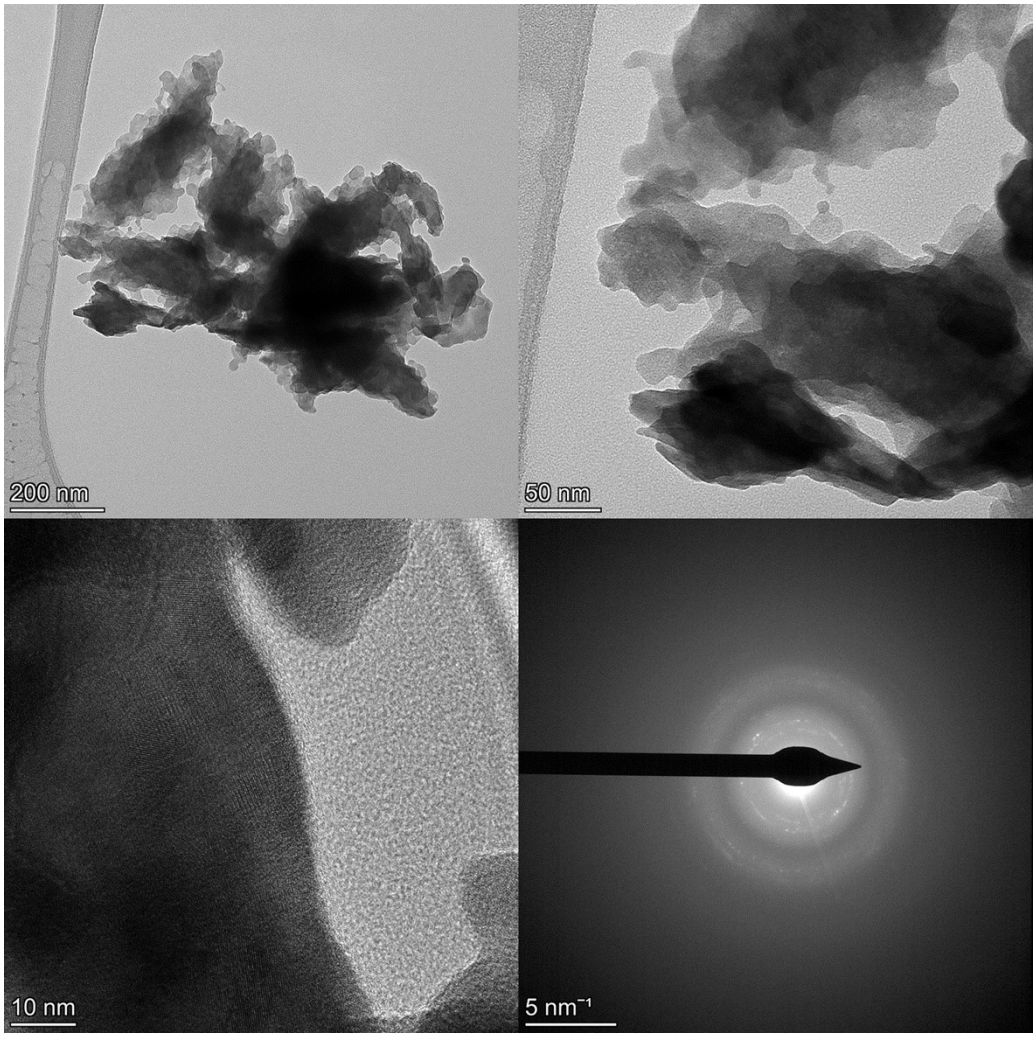

Figure 1: Transmission electron microscopy (TEM) images of a particle in different magnifications and its selected area electron diffraction (SAED) diffractogram

EXAFS fits of the HEF

Results from Metal K-edge EXAFS fitted parameters, including scattering paths, interatomic distance (R), interatomic distance from the model (R_{eff}), Debye Waller factor (σ^2), amplitude reduction factor (S_O^2), energy shift parameter (ΔE), and R-factor are listed below. The coordination number/ degeneracy (N) is listed with the appropriate model.

Table S4: Interatomic distances fitted on EXAFS Zr-K-edge spectra using a ZrF_4 previously used in sol-gel synthesised ZrF_4 materials.[1]

Zr K-edge

path	*N*	*σ²(Å²)*	*ΔR(Å)*	*R_{eff}(Å)*	*R(Å)*	*S_0^2*	*e_0(eV)*	*R-factor*
F3.1	2.000	0.00409	0.01148	2.03730	2.04878	0.880	-3.640	0.013
F2.1	2.000	0.00409	0.01148	2.08840	2.09987			
F1.1	2.000	0.00409	0.01148	2.14520	2.15667			
F3.2	2.000	0.00409	0.01148	2.19150	2.20297			
F2.3	2.000	0.00843	-0.17309	3.61320	3.44011			
Zr1.1	1.000	0.00248	0.01417	3.59720	3.61137			

Table S5: Interatomic distances fitted on EXAFS Zn-K-edge spectra using the ICSD entry 14146.

Zn K-edge

path	*N*	*σ²(Å²)*	*ΔR(Å)*	*R_{eff}(Å)*	*R(Å)*	*S_0^2*	*e_0(eV)*	*R-factor*
F1.1	6.000	0.00372	0.01932	2.03350	2.05282			
Zn1.1	2.000	0.02241	0.27376	3.13350	3.40726	0.646	3.684	0.027
F1.3	4.000	0.02241	0.27376	3.57460	3.84836			

Table S6: Interatomic distances fitted on EXAFS Ni-K-edge spectra using the ICSD entry 14145.

Ni K-edge

path	*N*	*σ²(Å²)*	*ΔR(Å)*	*R_{eff}(Å)*	*R(Å)*	*S_0^2*	*e_0(eV)*	*R-factor*
F1.1	2.000	-0.00517	-0.03698	1.98620	1.94921	0.635	-3.519	0.016
F1.2	3.000	-0.00309	0.07564	2.01820	2.09384			
Ni1.1	1.000	0.00257	0.27765	3.08360	3.36125			
F1.3	4.000	0.00257	0.27765	3.53690	3.81455			

Table S7: Interatomic distances fitted on EXAFS Mn-K-edge spectra using the ICSD entry 14142.

Mn K-edge

path	*N*	*σ²(Å²)*	*ΔR(Å)*	*R_{eff}(Å)*	*R(Å)*	*S_0^2*	*e_0(eV)*	*R-factor*
F1.1	6.000	0.00656	-0.01741	2.12200	2.10459	0.732	-1.804	0.008

Table S8: Interatomic distances fitted on EXAFS Fe-K-edge spectra using the materials project entry.

Fe K-edge

path	*N*	*σ²(Å²)*	*ΔR(Å)*	R_{eff}*(Å)*	*R(Å)*	S_0^2	e_0*(eV)*	*R-factor*
F1.1	6.000	0.00634	0.02390	1.92310	1.94700			
F1.1 F1.1	24.000	0.01560	0.15804	3.28290	3.44094			
Fe1.1	6.000	0.00999	0.10123	3.73260	3.83383			
F1.1 Fe1.1	12.000	0.01560	0.15804	3.78940	3.94744			
F1.2	6.000	0.04265	-0.33273	3.84430	3.51157	0.637	-0.828	0.018
F1.1 F1.1	6.000	0.01560	0.15804	3.84620	4.00424			
F1.1	6.000	0.01560	0.15804	3.84620	4.00424			
F1.3	6.000	0.04265	-0.33273	3.95780	3.62507			
F1.4	6.000	0.04265	-0.33273	4.42690	4.09417			

Table S9: Interatomic distances fitted on EXAFS Co-K-edge spectra using the ICSD entry 14144.

Co K-edge

path	*N*	*σ²(Å²)*	*ΔR(Å)*	R_{eff}*(Å)*	*R(Å)*	S_0^2	e_0*(eV)*	*R-factor*
F1.1	6.000	0.00781	0.01808	2.04140	2.05947			
Co1.1	2.000	0.02842	-0.19038	3.17960	2.98922			
F1.3	4.000	0.02842	-0.19038	3.56110	3.37072			
Co1.2	8.000	0.02842	-0.19038	3.68100	3.49062			
F1.4	4.000	0.02842	-0.19038	3.77330	3.58292	0.715	1.103	0.015
F1.5	8.000	0.01280	-0.46731	4.20450	3.73719			
F1.1 Co1.2	16.000	-0.00113	0.21539	3.87950	4.09489			
F1.1 F1.1	6.000	-0.00113	0.21539	4.08270	4.29809			
F1.2 F1.3	16.000	-0.00113	0.21539	4.24540	4.46079			
F1.2 F1.4	16.000	-0.00113	0.21539	4.35150	4.56689			

LSV of the single metallic fluorides

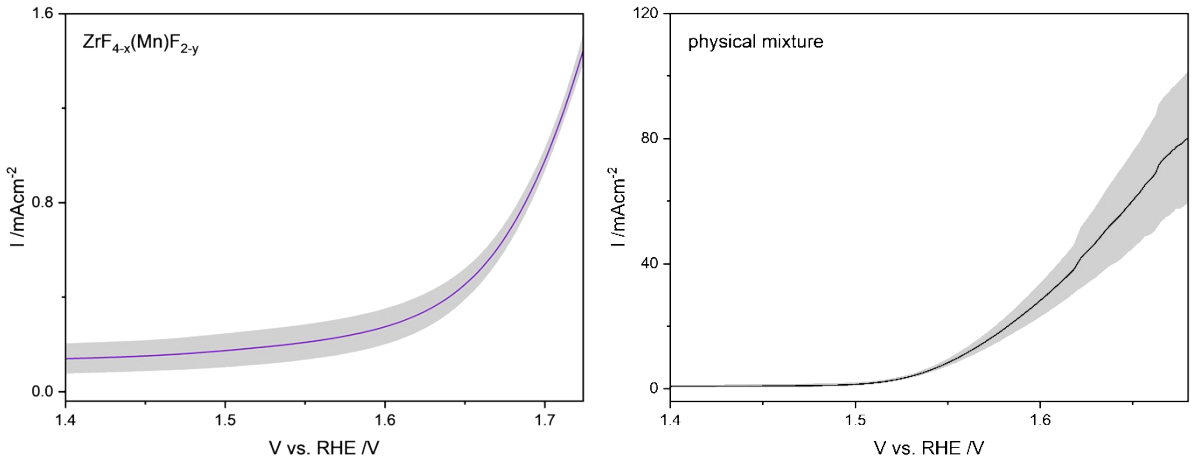

Figure 2: Linear Sweep voltommatry of the single metallic Mn (left) fluoride and a physical mixture of all single metallic fluorides (right).

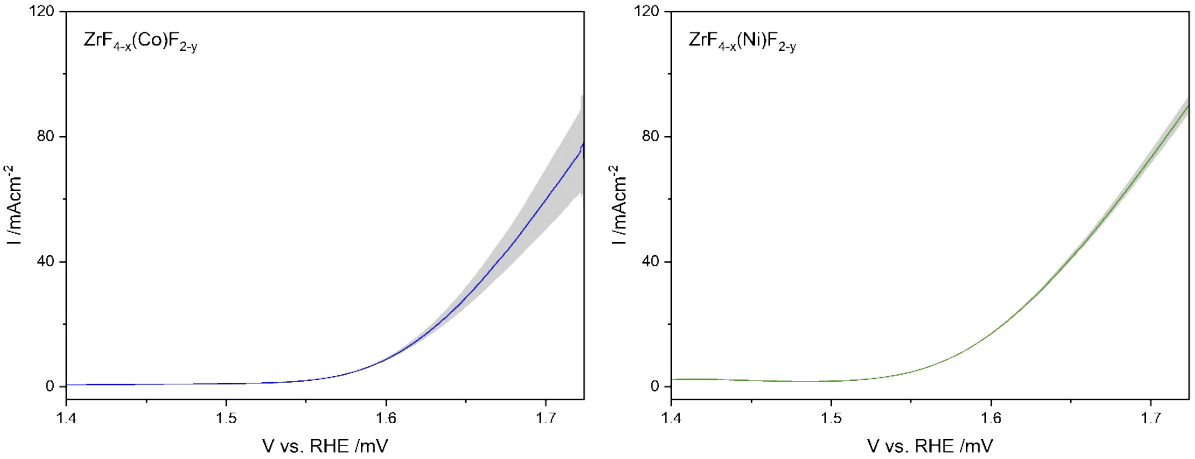

Figure 3: Linear Sweep voltommatry of the single metallic Co (left) and Ni (right) fluoride.

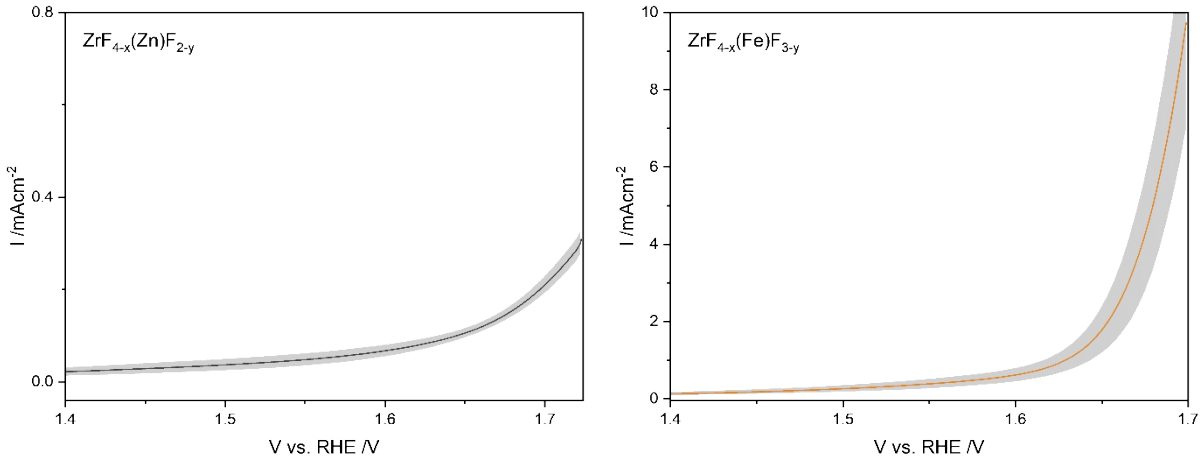

Figure 4: Linear Sweep voltammetry of the single metallic Zn (left) and Fe (right) fluoride.

Ex-situ XAS data

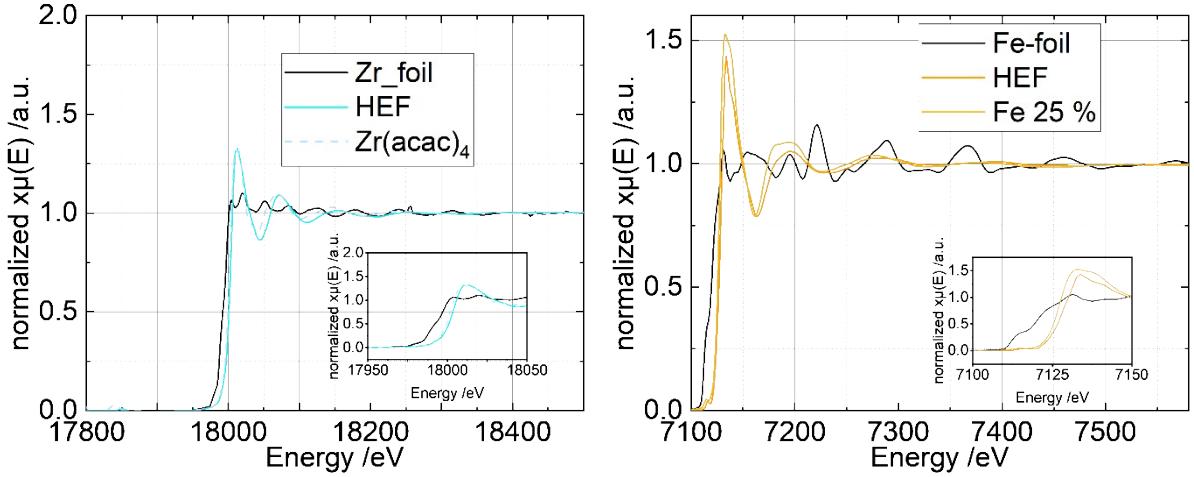

Figure 5: Normalised X-ray Absorption spectroscopy data at the Zr (left) and Fe (right) K-edge.

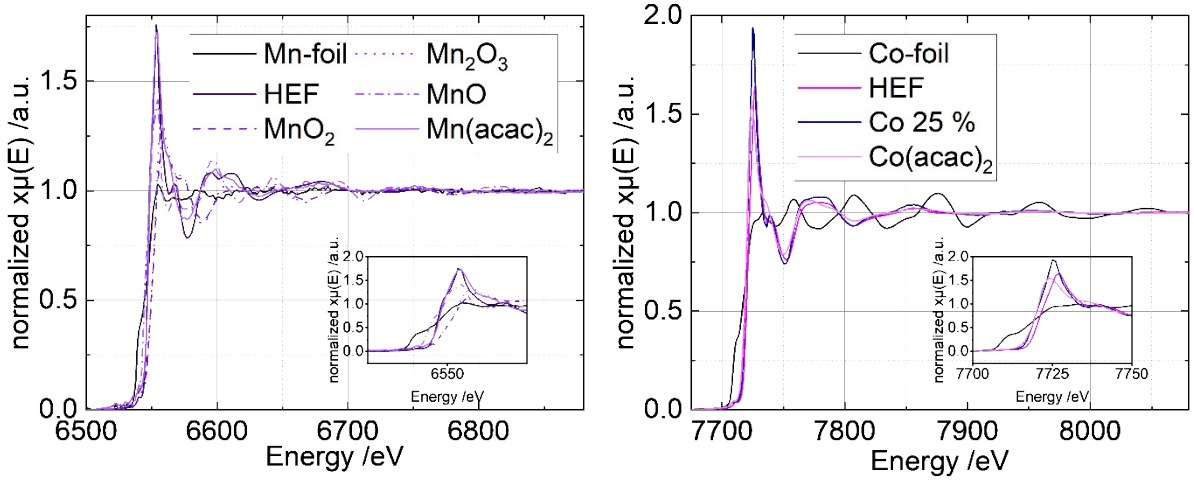

Figure 6:: Normalised X-ray Absorption spectroscopy data at the Mn (left) and Co (right) K-edge.

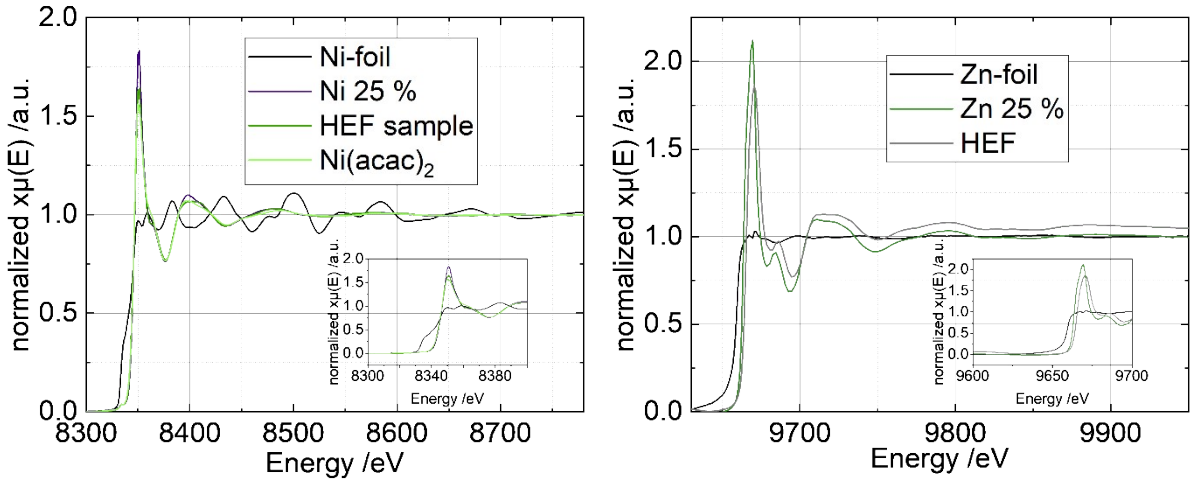

Figure 7:: Normalised X-ray Absorption spectroscopy data at the Ni (left) and Zn (right) K-edge.

XRD patterns of the single metallic fluorides

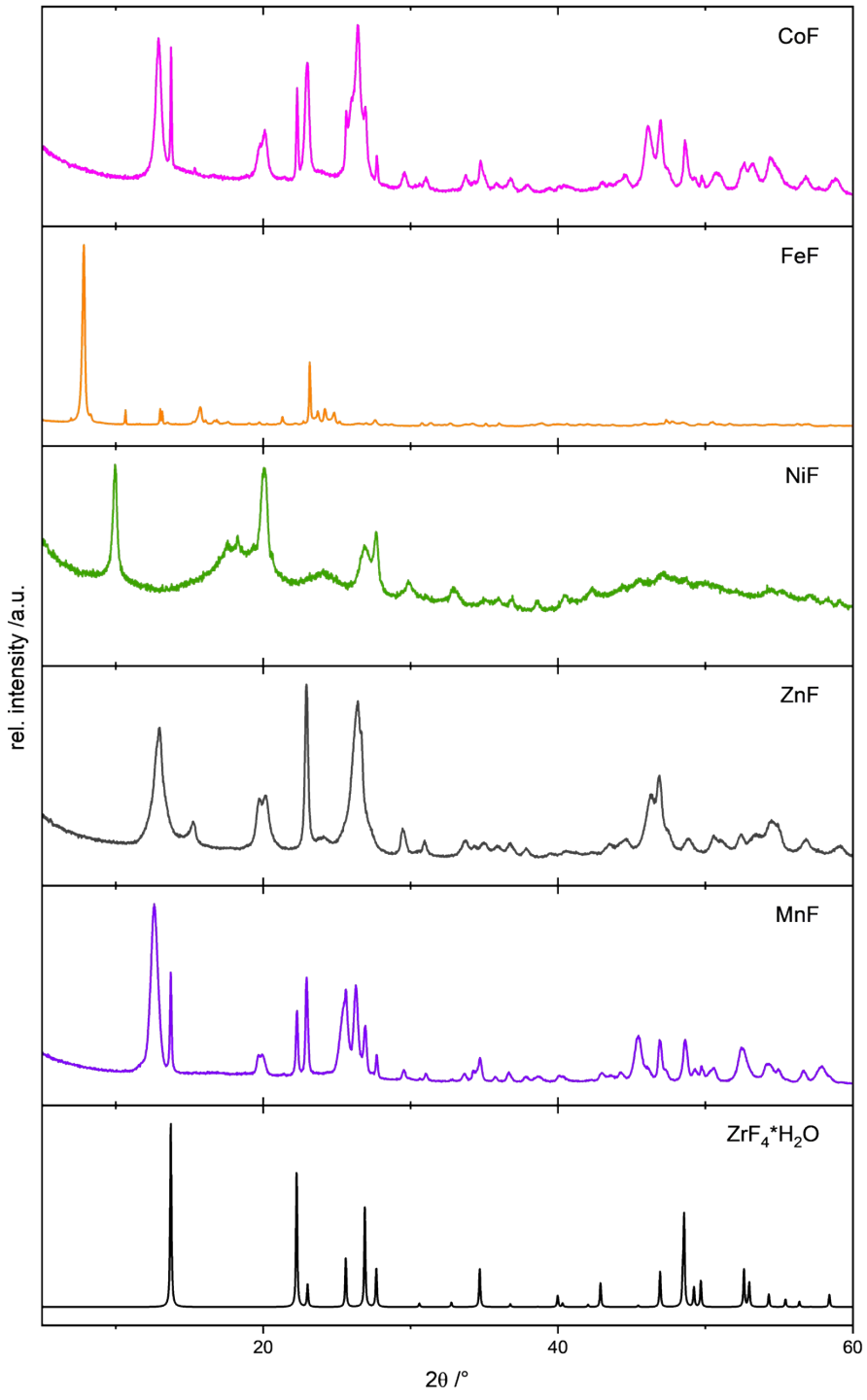

Figure 8: Ex-situ XRD patterns of the single metallic fluorides on the ZrF_4 support. The pattern of ZrF_4*H_2O is displayed as a reference.[2]

XRD pattern of the bimetallic NiCo fluoride

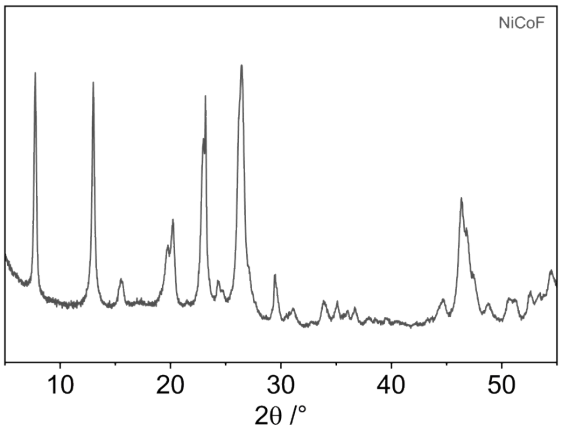

Figure 9: Ex-situ XRD patterns of the Ni-Co-bimetallic fluoride on the ZrF4 support

XRDs of ZrF supports

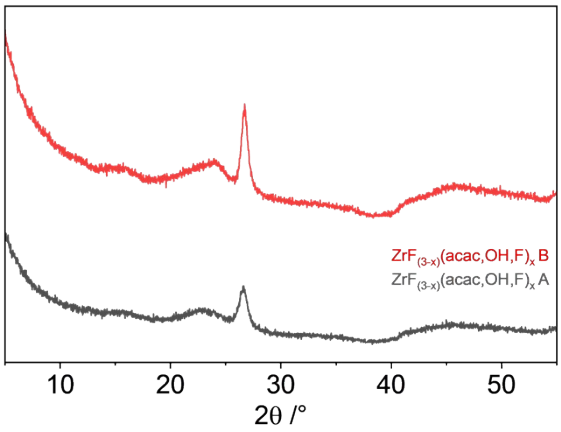

Figure 10: XRD pattern of the ZrF supports, where B has additionally been heated to 80 °C for 10 min.

Magnitude plots of χ(R) of the Fe samples and precursor

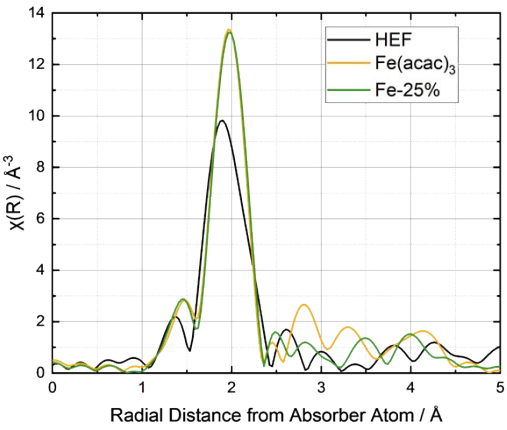

Figure 11: The Magnitude plots of the χ(R) of the HEF, the Fe(acac)3 precursor and single metallic Fe sample.

Reciprocal space data of the total scattering experiment of the HEF

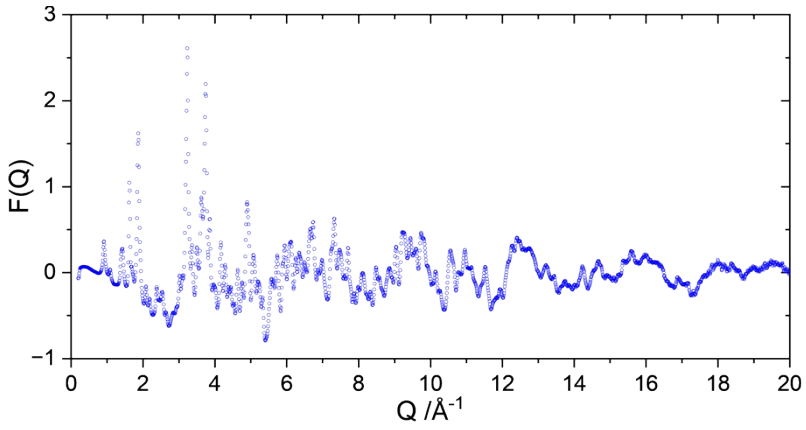

Figure 12: Reciprocal space data of the total scattering experiment of the HEF.

Infrared spectra of the single metallic and HE fluorides

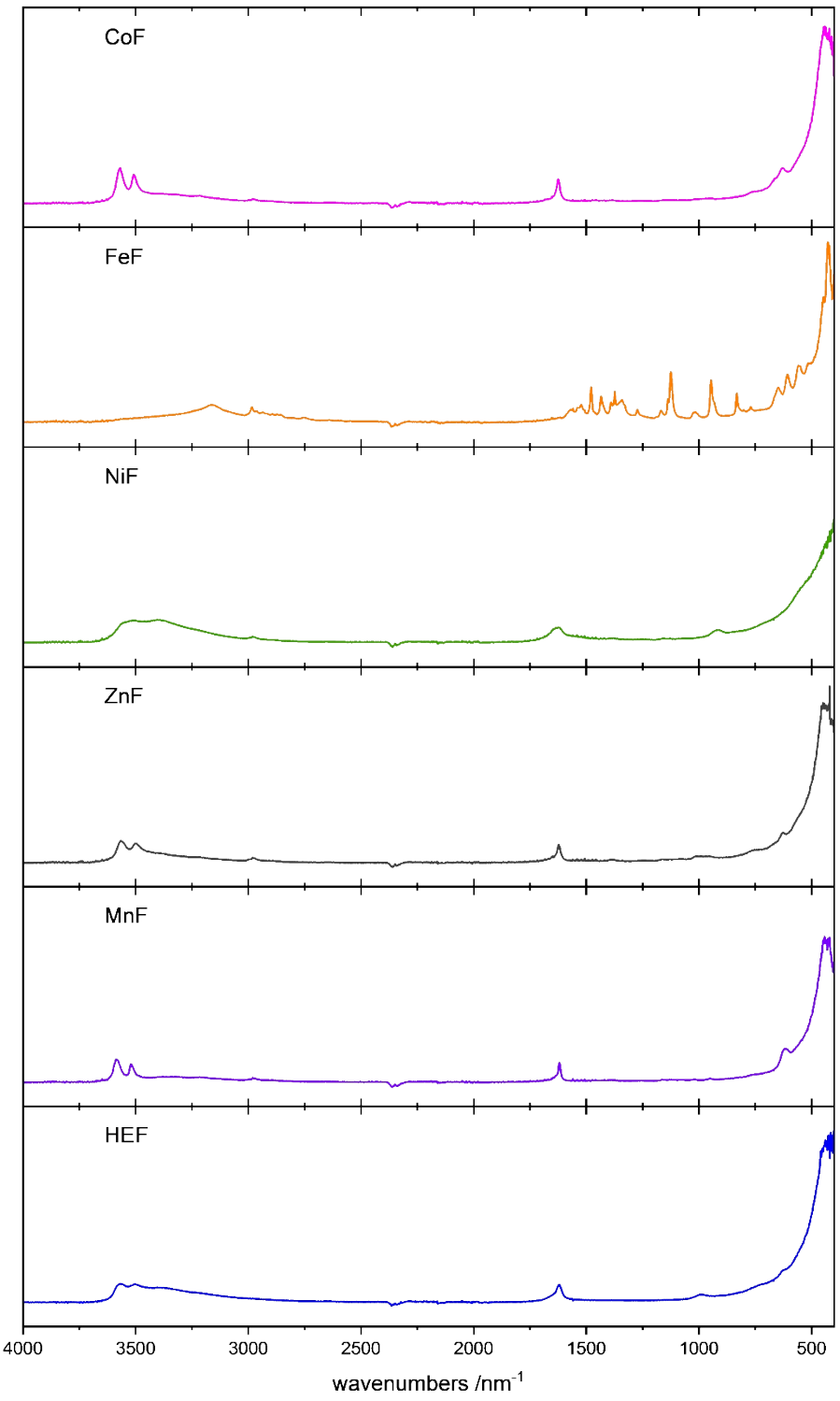

Figure 13: IR spectra obtained from the single metallic and the HE fluorides on the ZrF_4 support.

Thermogravimetric analysis (TGA) and differential scanning calorimetrie (DSC) traces of the fluorides

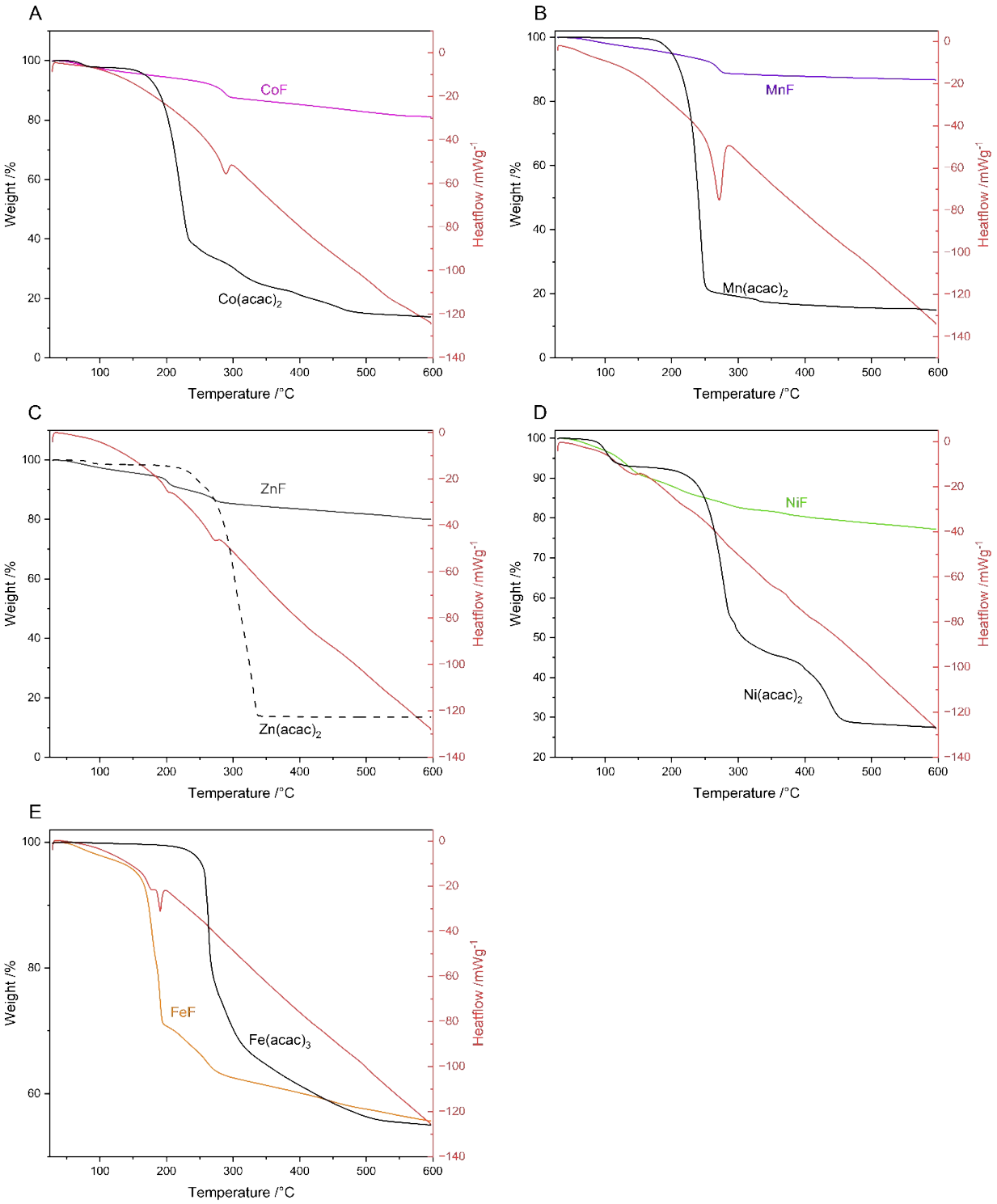

Figure S 1: TGA/DSC traces (red) from the single metallic fluorides on the ZrF support and their respective acetylacetonate or acetate (black). The TGA can show that the observed weight losses do not correspond to now reacted reagents. Hence, a conversion to the respective fluorinated species is not contradictory to the TGA findings.

References

1 C. Heinekamp, S. Kneiske, A. Guilherme Buzanich, M. Ahrens, T. Braun and F. Emmerling, *Catal. Sci. Technol.*, 2024, **14**, 673–680.

2 B. Kojić-Prodić, F. Gabela, Ž. Ružić-Toroš and M. Šljukić, *Acta Crystallogr. B*, 1981, **37**, 1963–1965.